Optimal Voltage Control Using an Equivalent Model of a Low-Voltage Network Accommodating Inverter-Interfaced Distributed Generators

Mu-Gu Jeong [1], Young-Jin Kim [2], Seung-Il Moon [1] and Pyeong-Ik Hwang [3],*

[1] Department of Electrical and Computer Engineering, Seoul National University, 1 Gwanak-ro, Gwanak-gu, Seoul 08826, Korea; mugujeong88@gmail.com (M.-G.J.); moonsi@plaza.snu.ac.kr (S.-I.M.)

[2] Department of Electrical Engineering, Pohang University of Science and Technology, 77 Cheongam-ro, Nam-gu, Pohang 37673, Korea; powersys@postech.ac.kr

[3] Department of Electrical Engineering, Chosun University, 309 Pilmun-daero, Dong-gu, Gwangju 61452, Korea

* Correspondence: hpi@chosun.ac.kr; Tel.: +82-62-230-7033

Abstract: The penetration of inverter-based distributed generators (DGs), which can control their reactive power outputs, has increased for low-voltage (LV) systems. The power outputs of DGs affect the voltage and power flow of both LV and medium-voltage (MV) systems that are connected to the LV system. Therefore, the effects of DGs should be considered in the volt/var optimization (VVO) problem of LV and MV systems. However, it is inefficient to utilize a detailed LV system model in the VVO problem because the size of the VVO problem is increased owing to the detailed LV system models. Therefore, in order to formulate and solve the VVO problem in an efficient way, in this paper, a new equivalent model for an LV system including inverter-based DGs is proposed. The proposed model is developed based on an analytical approach rather than a heuristic-fitting one, and it therefore enables the VVO problem to be solved using a deterministic algorithm (e.g., interior point method). In addition, a method to utilize the proposed model for the VVO problem is presented. In the case study, the results verify that the computational burden to solve the VVO problem is significantly reduced without loss of accuracy by the proposed model.

1. Introduction

Owing to opposition to the installation of new transmission facilities and the environmental issues associated with large-scale nuclear and thermal plants, a distributed generator (DG) is emerging as an alternative power source in distribution systems. Although DGs offer a variety of economic and technical benefits [1], a high penetration of DGs results in new problems for the distribution system operation, such as voltage rise [2,3]. Therefore, various volt/var optimization (VVO) methods that consider DGs and that utilize DGs as a controllable resource have been proposed for medium-voltage (MV) distribution systems (e.g., 1 kV < V_{MV} < 100 kV) [4–7]. Using these proposed methods, the active power loss and switching operation of the on-load tap changers (OLTCs) and shunt capacitors can be reduced while maintaining the voltages within their operational bounds.

Meanwhile, the penetration of small-size DGs in low-voltage (LV) distribution systems (e.g., V_{LV} < 1 kV) has gradually increased. For example, 70% of the capacity of photovoltaic (PV) generators in Germany is installed in LV systems [8]. The DGs in LV systems change the power flow not only in LV systems but also in MV systems [9,10]. Therefore, in order to ensure the stable and economic operation

of both MV and LV systems, the DGs should be considered for distribution system operation, and should be utilized as reactive power sources if the DGs can control their reactive power outputs. For this reason, the German grid codes require the reactive power control capability for the PV generation, where the rated capacity is larger than 3.68 kVA, connected to the LV distribution systems [11,12].

In order to utilize DGs in LV systems for the VVO of both LV and MV systems, detailed models of all the relevant LV systems need to be included for the VVO problem. Moreover, if the DGs are renewable resources, a stochastic optimization method should be used to consider the uncertainty of the active power output. One of the stochastic methods is the scenario-based method [13–15]. In the scenario-based methods, many scenarios that have own fixed active power profiles are generated based on probability density functions. Then, the final optimal solution is determined from the optimal solutions of the VVO problems for all scenarios. Therefore, if the detailed models of the LV systems are used for the VVO, the increase in the number of variables of the VVO problem significantly increases the size of the optimization problem and computational burden.

One method for reducing the problem size is to utilize an equivalent model that can replace the detailed LV system model. Various equivalent models have been proposed for the analysis of transmission and distribution systems. The simplest model is the single-bus equivalent model, such as the active and reactive power (PQ) bus model, which represents systems with constant active and reactive injections, and the Thevenin equivalent circuit, which represents systems with constant-voltage phasor and series impedances. To increase the accuracy of the model, the Ward injection model and the radial equivalent independent (REI) model were proposed [16,17]. In the Ward injection model, the system is reduced to the equivalent power injection and admittance using the Gauss elimination method. In the REI model, the system is transformed into a simplified radial system with a virtual node, based on the injection powers and voltages in the equivalent area. Recently, new methods to aggregate loads in distribution system considering demand side management and microgeneration were proposed [18,19]. For analyzing the LV system with DGs briefly, the sensitivity-based model of LV systems are proposed in [20]. An equivalent model for a distribution system with a high penetration of PV systems was proposed in [21]. In the model, the injection power at the boundary bus is given as an equation of the total active power generation, power factor of the generators, and total power consumption of loads in the system. The coefficients of the equation are obtained from data processing that minimizes the squared error between the calculated values using the model and the actual value. In [22], an equivalent model that includes the network power loss was presented, with consideration given to the DG outputs. The reactive power of the DGs is modeled as pre-determined values. Because the network power loss is represented as a black box, the model can only be adopted for heuristic algorithms (e.g., particle-swarm optimization). In summary, in these models, the variation of the network power losses and voltages due to the reactive power control of the DGs is not represented, and they therefore cannot be employed for VVOs that utilize the DGs as controllable resources.

In this paper, a new analytical equivalent model for an LV system is proposed considering the effect of reactive power control of DGs on the network power losses and voltages. The proposed model can be utilized to realize VVO for both MV and LV systems considering the reactive power control of the DGs. Moreover, the proposed model can be adopted to VVO using deterministic optimization methods, which are generally faster and more stable than heuristic methods [23], because it is an analytical model. Section 2 describes the proposed equivalent model of the LV system, which consists of three components that represent: (a) the equivalent reactive power source (ERPS); (b) LV power loss; and (c) residual power injection. In Section 3, the utilization method of the proposed model for a VVO based on a deterministic method is presented. The VVO problem is to minimize the weighted sum of the total power loss and the number of switching operations of voltage-regulating devices. In Section 4, the accuracy of the proposed model is verified by comparing the results of the proposed model with those of the detailed model. In addition, the effects of the proposed model on the VVO are also validated. Finally, Section 5 concludes the paper.

2. Equivalent Model for Low-Voltage Distribution System with Distributed Generators

Figure 1 shows the proposed equivalent model of an LV distribution system including the DGs. The LV system is modeled as a single-bus system connected to three components: (a) the ERPS; (b) LV power loss; and (c) residual power injection. The ERPS represents the aggregated reactive power outputs of the DGs, which is adjusted by the VVO, in the LV system. The LV power loss consists of the network power loss and the inverter power loss of the DG itself. The residual power injection refers to the components that remain after the ERPS modeling and the power loss calculation, i.e., the active and reactive power consumption of the loads and the active power output of the DGs. Because the voltages of LV systems vary according to the reactive power output of the DGs, the LV power loss and the residual power injection are modeled as a function of the reactive power of the ERPS.
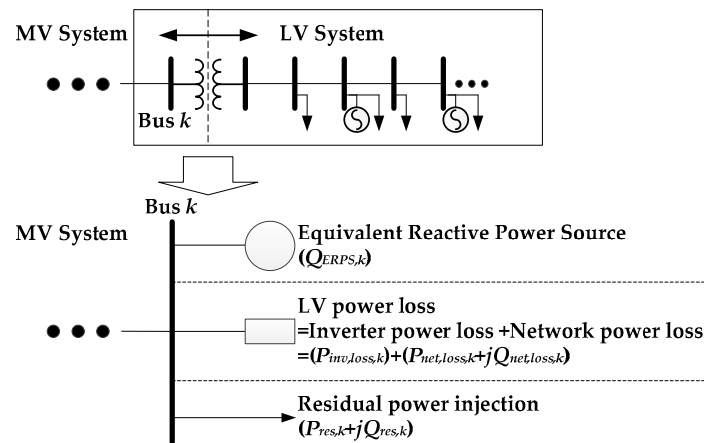

Figure 1. Proposed model for a low-voltage (LV) system.

2.1. Equivalent Reactive Power Source (ERPS)

The reactive power output of the ERPS is the total reactive power output of all the DGs in the corresponding LV system. In the VVO problem with the proposed equivalent model, the LV system is represented as a single bus, as shown in Figure 1, and only the reactive power output of the ERPS is the decision variable for the VVO problem. Because the reactive power outputs of the DGs are limited, the reactive power limits of the ERPS should be determined. The minimum and maximum reactive power outputs of the ERPS are given by the sum of the reactive power limits of all DGs in the LV system:

$$Q_{ERPS,\min,k}^t = -Q_{ERPS,\max,k}^t = -\sum_{i=1}^{N_{LV,DG,k}} Q_{DG,\max,k,i}^t, \tag{1}$$

where $Q_{DG,\max,k,i}^t = \sqrt{\left(S_{rated,k,i}\right)^2 - \left(P_{DG,k,i}^t\right)^2}$ [24].

After determining the reactive power reference of the ERPS by solving the VVO problem, the reactive power reference for each DG is determined in proportion to its reactive power capacities as follows:

$$Q_{DG,k,i}^t = \frac{Q_{DG,\max,k,i}^t - Q_{DG,\min,k,i}^t}{\displaystyle\sum_{i=1}^{N_{LV,DG,k}} Q_{DG,\max,k,i}^t - \sum_{i=1}^{N_{LV,DG,k}} Q_{DG,\min,k,i}^t} Q_{ERPS,k}^t = \alpha_{k,i}^t Q_{ERPS,k}^t. \tag{2}$$

By adopting the distribution method, some DGs can be prevented from reaching their capacity limits more rapidly than others.

2.2. Low-Voltage Power Loss

The total power loss in an LV system comprises the inverter power loss and the network power loss.

2.2.1. Inverter Power Loss

The inverter power loss of a DG that is connected to the LV Bus i of an MV Bus k can be formulated as a quadratic function of the apparent power output of the DG as follows [25,26]:

$$P_{inv,loss,k,i}^t = c_{inv,0,k,i} S_{rated,k,i} + c_{inv,1,k,i} S_{DG,k,i}^t + \frac{c_{inv,2,k,i}}{S_{rated,k,i}} \left(S_{DG,k,i}^t\right)^2. \tag{3}$$

To simplify (3) as a polynomial function of the reactive power references of the DG, a quadratic Lagrange polynomial is utilized [27], i.e., the inverter power loss is obtained by substituting (2) into the quadratic Lagrange polynomial. Finally, the total inverter power loss of the LV system connected to the MV Bus k is derived by summing the inverter power losses of all the DGs in the LV system, resulting in:

$$P_{inv,loss,k}^t = D_{inv,0,k}^t + D_{inv,1,k}^t \left|Q_{ERPS,k}^t\right| + D_{inv,2,k}^t \left(Q_{ERPS,k}^t\right)^2. \tag{4}$$

The detailed process employed to obtain $D_{inv,0,k}^t$, $D_{inv,1,k}^t$, and $D_{inv,2,k}^t$ is described in Appendix A.

2.2.2. Network Power Loss

The network power loss depends on the network topology, the line impedance, the bus injection power, and the bus voltage. Because the bus injection powers and bus voltages of the LV system vary according to the VVO results, while others remain unchanged, it is necessary to estimate the bus injection powers and the voltages to calculate the network power loss in the LV system.

The bus injection powers and the voltages can be estimated from the variations between the initial operating point and the operating point after a control action. In order to distinguish the initial operating point used for the VVO problem, in this paper, the initial operating point for the estimation is referred to as the base operating point. The subscription for the base operating point is *base*. To improve the accuracy of the VVO solution, the base operating point should be updated in the procedure for solving the VVO problem. The updating method is described in Section 3.

The bus injection power comprises the power consumption of a load and the power generation of a DG. Because the load demand varies with the bus voltage, the variation should be considered to calculate the network power loss. One of the widely used models to express the static load demand characteristic depending on the voltage magnitude is the constant impedance-current-power (ZIP) model [28,29]. Using the ZIP model, the active and reactive power consumptions of the load at LV bus i are expressed as:

$$P_{Load,k,i} = \sum_{\beta=0}^{2} P_{L,norm,k,i} K_{P,k,i,\beta} V_{LV,k,i}^{\beta}, \tag{5}$$

$$Q_{Load,k,i} = \sum_{\beta=0}^{2} Q_{L,norm,k,i} K_{Q,k,i,\beta} V_{LV,k,i}^{\beta}, \tag{6}$$

where β = 0 (constant power), 1 (constant current), 2 (constant impedance). Meanwhile, it can be assumed that the active power of the DG does not change because the variation of the inverter active power loss due to the reactive power adjustment is much smaller than the total power output of the DG.

Consequently, the active power injection of the LV bus i can be approximated to:

$$P_{LV,k,i}^t \approx P_{DG,inv,k,i,base}^t - \sum_{\beta=0}^{2} P_{L,norm,k,i}^t K_{P,k,i,\beta}^t V_{LV,k,i}^{t\ \beta}, \tag{7}$$

where $P_{DG,inv,k,i,base}^t = P_{DG,k,i}^t - P_{inv,loss,k,i,base}^t$. $P_{inv,loss,k,i,base}^t$ is derived by (3). Because the reactive power of the DG is determined by (2) and the reactive power of the load is changed by (6), the reactive power injection of LV bus i given by:

$$Q_{LV,k,i}^t = \alpha_{k,i}^t Q_{ERPS,k}^t - \sum_{\beta=0}^{2} Q_{L,norm,k,i}^t K_{Q,k,i,\beta}^t V_{LV,k,i}^{t\ \beta}. \tag{8}$$

According to the results of the VVO, the voltage magnitudes of an LV system are mainly changed owing to two factors, i.e., the reactive variations of the DGs in the LV system and the voltage magnitude variation of the MV bus connected to the LV system. Because the LV system is downstream of the MV bus, the voltage magnitude variations in the LV buses are almost identical to that of the MV bus [30]. Therefore, it can be assumed that the voltage magnitude variations of the LV buses are almost identical to that of the MV bus if the active and reactive power outputs of the DGs are not changed. Meanwhile, the voltage magnitude variation of LV buses due to the reactive power control of the DGs can be approximated using the bus voltage magnitude sensitivity with respect to the reactive power injection. Because the reactive power of each DG is determined from the reactive power output of ERPS using (2), the voltage magnitude variation can be expressed as a function of the reactive power output of the ERPS. Consequently, the voltage magnitude variation is approximated as follows:

$$V_{LV,k,i}^t \approx V_{LV,k,base}^t + H_{VQ,k,i}^t \left(Q_{ERPS,k}^t - Q_{ERPS,k,base}^t \right) + \left(V_{MV,k}^t - V_{MV,k,base}^t \right) \tag{9}$$

where $H_{VQ,k,i}^t$ is the voltage magnitude sensitivity with respect to the reactive power of the ERPS. In Appendix B, the detailed process of the equation development is explained. The second term corresponds to the variations that are due to the reactive power control of DGs, while the last one refers to the variation due to the voltage magnitude change of the MV bus.

Based on the bus injection powers and voltages obtained, the network power loss is estimated as follows. Using the bus admittance matrix, the injected bus current can be represented as a function of the bus voltage:

$$\begin{bmatrix} I_{MV,k}^t \\ \mathbf{I_{LV,k}^t} \end{bmatrix} = \begin{bmatrix} Y_{1,k} & \mathbf{Y_{2,k}}^T \\ \mathbf{Y_{2,k}} & \mathbf{Y_{3,k}} \end{bmatrix} \begin{bmatrix} E_{MV,k}^t \\ \mathbf{E_{LV,k}^t} \end{bmatrix}. \tag{10}$$

From (10), the voltage of LV bus i and the total current injected into MV bus k are expressed as:

$$E_{LV,k,i}^t = \sum_{m=1}^{N_{LV,Bus,k}} C_{II,k,i,m} I_{LV,k,m}^t - E_{MV,k}^t \sum_{m=1}^{N_{LV,Bus,k}} C_{II,k,i,m} Y_{2,k,m}, \tag{11}$$

$$I_{MV,k}^t = C_{VV,k} E_{MV,k}^t + \sum_{m=1}^{N_{LV,Bus,k}} \sum_{i=1}^{N_{LV,Bus,k}} Y_{2,k,m} C_{II,k,m,i} I_{LV,k,i}^t. \tag{12}$$

where $C_{VV,k} = Y_{1,k} - \sum_{m=1}^{N_{LV,Bus,k}} \sum_{i=1}^{N_{LV,Bus,k}} Y_{2,k,m} C_{II,k,m,i} Y_{2,k,i}$. $C_{II,k,m,i}$ is the m-th row and i-th column element of the inverse matrix of $\mathbf{Y_{3,k}}$. Meanwhile, the network power loss in the LV system is expressed as the difference between the injected power from the MV system and the total power injections in the LV buses, i.e.,

$$S_{net.loss,k}^t = E_{MV,k}^t I_{MV,k}^{t\ *} + \sum_{i=1}^{N_{LV,Bus,k}} E_{LV,k,i}^t I_{LV,k,i}^{t\ *}. \tag{13}$$

Under normal operating conditions, the differences in the voltage angles of LV buses are relatively small [31,32], and the differences are negligible. Therefore, the network power loss equation given by (13) can be approximated as follows by using (11) and (12):

$$S^t_{net.loss,k} = C_{VV,k} {}^* V^t_{MV,k}{}^2 + V^t_{MV,k} \sum_{i=1}^{N_{LV,Bus,k}} C_{VI,k,i} \left(\frac{S^t_{LV,k,i}}{V^t_{LV,k,i}} \right) + \sum_{i=1}^{N_{LV,Bus,k}} \sum_{m=1}^{N_{LV,Bus,k}} C_{II,k,i,m} \left(\frac{S^t_{LV,k,i}}{V^t_{LV,k,i}} \right) \left(\frac{S^t_{LV,k,m}}{V^t_{LV,k,m}} {}^* \right). \tag{14}$$

Appendix C provides the detailed process for obtaining (14). Finally, the network power loss is formulated as an analytic function of the reactive output power of the ERPS and the voltage magnitude of the MV bus by using (7)–(9) and applying the Taylor series:

$$
\begin{aligned}
P^t_{net.loss,k} + jQ^t_{net.loss,k} &= \left(D^t_{net,0,k} + D^t_{net,1,k} Q^t_{ERPS,k} + D^t_{net,2,k} Q^t_{ERPS,k}{}^2 + D^t_{net,3,k} Q^t_{ERPS,k}{}^3 + D^t_{net,4,k} Q^t_{ERPS,k}{}^4 \right) \\
&+ \left(D^t_{net,5,k} + D^t_{net,6,k} Q^t_{ERPS,k} + D^t_{net,7,k} Q^t_{ERPS,k}{}^2 + D^t_{net,8,k} Q^t_{ERPS,k}{}^3 \right) V^t_{MV,k} \\
&+ \left(D^t_{net,9,k} + D^t_{net,10,k} Q^t_{ERPS,k} + D^t_{net,11,k} Q^t_{ERPS,k}{}^2 \right) V^t_{MV,k}{}^2
\end{aligned} \tag{15}
$$

The detailed process of acquiring $D^t_{net,0,k}$–$D^t_{net,11,k}$ is explained in Appendix C.

2.3. Residual Power Injection

The LV system components that remain after modeling the ERPS and calculating the power loss are aggregated to the residual power injection, $P^t_{res,k} + jQ^t_{res,k}$. In order words, the residual power injection corresponds to the active and reactive power consumption of loads and the active power output of the DGs. Using the ZIP model given by (5) and (6) for a load, the residual power injection is obtained as follows:

$$P^t_{res,k} = \sum_{i=1}^{N_{LV,Bus,k}} \sum_{\beta=0}^{2} P^t_{L,norm,k,i} K^t_{P,k,i,\beta} V^t_{LV,k,i}{}^\beta - \sum_{i=1}^{N_{LV,DG,k}} P^t_{DG,k,i}, \tag{16}$$

$$Q^t_{res,k} = \sum_{i=1}^{N_{LV,Bus,k}} \sum_{\beta=0}^{2} Q^t_{L,norm,k,i} K^t_{Q,k,i,\beta} V^t_{LV,k,i}{}^\beta. \tag{17}$$

By substituting the voltage magnitude that is estimated by using (9), the residual power injection can be approximated as:

$$P^t_{res,k} + jQ^t_{res,k} \approx D^t_{res,0,k} + D^t_{res,1,k} Q^t_{ERPS,k} + D^t_{res,2,k} Q^t_{ERPS,k}{}^2 + (D^t_{res,3,k} + D^t_{res,4,k} Q^t_{ERPS,k}) V^t_{MV,k} + D^t_{res,5,k} V^t_{MV,k}{}^2, \tag{18}$$

where:

$$D^t_{res,0,k} = \sum_{i=1}^{N_{LV,Bus,k}} \sum_{\beta=0}^{2} d^t_{res,1,k,i,\beta} d^t_{res,2,k,i}{}^\beta - \sum_{i=1}^{N_{LV,DG,k}} P^t_{DG,k,i}, \quad D^t_{res,1,k} = \sum_{i=1}^{N_{LV,Bus,k}} \sum_{\beta=0}^{2} \beta d^t_{res,1,k,i,\beta} H^t_{VQ,k,i} d^t_{res,2,k,i}{}^{\beta-1},$$

$$D^t_{res,2,k} = \sum_{i=1}^{N_{LV,DG,k}} d^t_{res,1,k,i,2} H^t_{VQ,k,i}{}^2, \quad D^t_{res,3,k} = \sum_{i=1}^{N_{LV,Bus,k}} \sum_{\beta=0}^{2} \beta d^t_{res,1,k,i,\beta} d^t_{res,2,k,i}{}^{\beta-1}, \quad D^t_{res,4,k} = \sum_{i=1}^{N_{LV,DG,k}} 2 d^t_{res,1,k,i,2} H^t_{VQ,k,i},$$

$$D^t_{res,5,k} = \sum_{i=1}^{N_{LV,DG,k}} d^t_{res,1,k,i,2}, \quad d^t_{res,1,k,i,\beta} = P^t_{L,norm,k,i} K^t_{P,k,i,\beta} + jQ^t_{L,norm,k,i} K^t_{Q,k,i,\beta},$$

$$d^t_{res,2,k,i} = V^t_{LV,k,base} - H^t_{VQ,k,i} Q^t_{ERPS,k,base} - V^t_{MV,k,base}.$$

3. Application to Volt/Var Optimization Problem Formulation

In the proposed equivalent model explained in Section 2, the LV distribution system, including the inverter-interfaced DGs, is expressed as the analytic function of the voltage magnitude of the MV bus, which is connected to the LV system, and the reactive power output of the ERPS. Therefore, the model can be easily adopted for the formulation of the VVO problem for MV and LV systems, considering the

power loss and voltage in the LV systems. In this section, a method to apply the proposed equivalent model to a general VVO problem is presented. The VVO is performed to determine one-day operation schedules for the volt/var control devices, including DGs that are connected to the LV system.

For the VVO problem, several objective functions have been considered, such as those presented in [33,34]; in particular, the term corresponding to the network power loss has been commonly included in the objective function. In this paper, the number of switching operations of the OLTC and the shunt capacitors are also considered to prevent their frequent switching, which can increase maintenance cost [5]. Therefore, the objective function is set to the weighted sum of the active power loss and the number of switching operations with the cost-weighting factors:

$$\min \sum_{t=1}^{24} \left(w_P \left(P_{MV,loss}^t + \sum_{k=1}^{N_{LV,sys}} \left(P_{inv,loss,k}^t + P_{net,loss,k}^t \right) \right) + w_{tap} \left| tap^{t+1} - tap^t \right| + \sum_{l=1}^{N_{sh}} w_{sh,l} \left| sh_l^{t+1} - sh_l^t \right| \right). \quad (19)$$

The weighting factors may be differently determined by the distribution system operator [5,35] depending on the target network conditions.

The equality constraints for the VVO problem are the power balance constraints, as follows:

$$P_{MV,k}^t = \sum_{n=1}^{N_{MV,Bus}} V_{MV,k}^t V_{MV,n}^t \left(G_{MV,k,n} \cos \left(\theta_{MV,k}^t - \theta_{MV,n}^t \right) + B_{MV,k,n} \sin \left(\theta_{MV,k}^t - \theta_{MV,n}^t \right) \right), \quad (20)$$

$$Q_{MV,k}^t = \sum_{n=1}^{N_{MV,Bus}} V_{MV,k}^t V_{MV,n}^t \left(G_{MV,k,n} \sin \left(\theta_{MV,k}^t - \theta_{MV,n}^t \right) - B_{MV,k,n} \cos \left(\theta_{MV,k}^t - \theta_{MV,n}^t \right) \right). \quad (21)$$

The active and reactive injection powers of MV bus *k* are determined using (4), (15), and (18), i.e.,

$$P_{MV,k}^t = -P_{inv,loss,k}^t - P_{net,loss,k}^t - P_{res,k}^t, \quad (22)$$

$$Q_{MV,k}^t = Q_{ERPS,k}^t - Q_{net,loss,k}^t - Q_{res,k}^t. \quad (23)$$

The conventional inequality constraints are as follows:

$$V_{MV,\min} \leq V_{MV,k}^t \leq V_{MV,\max}, \quad (24)$$

$$tap_{\min} \leq tap^t \leq tap_{\max}, \quad (25)$$

$$0 \leq sh_l^t \leq sh_{\max,l}. \quad (26)$$

The first inequality constraint indicates that the voltage magnitudes of MV buses should be maintained within their operational bounds. The others, (25) and (26), represent the maximum and minimum operational limits of the tap position of the OLTC and the number of shunt capacitors, respectively. Because the proposed VVO considers the voltages of the LV systems, the voltages can be maintained within their operational limits by introducing an appropriate inequality constraint. By using the voltage magnitude approximation given by (9), the inequality constraint for the voltage magnitudes of the LV buses is obtained:

$$\mathbf{U} V_{LV,\min,k} \leq \mathbf{V}_{\mathbf{LV,k,base}}^{\mathbf{t}} + \mathbf{H}_{\mathbf{VQ,k}}^{\mathbf{t}} \left(Q_{ERPS,k}^t - Q_{ERPS,k,base}^t \right) + \mathbf{U} (V_{MV,k}^t - V_{MV,k,base}^t) \leq \mathbf{U} V_{LV,\max,k}, \quad (27)$$

where **U** is the $(N_{LV,Bus,k} \times 1)$ vector composed of 1's. In addition, the reactive power limits of the ERPS are added as an inequality constraint:

$$Q_{ERPS,\min,k}^t \leq Q_{ERPS,k}^t \leq Q_{ERPS,\max,k}^t. \quad (28)$$

The VVO problem (19)–(28) is formulated using analytic equations; note that (4) and (19), which include the absolute value functions, can be transformed into analytic functions using the epigraph

problem form [36]. Therefore, the gradients and the Hessian that are used to solve the VVO problem can be defined, implying that the proposed equivalent model of the LV system enables the VVO problem to be solved using deterministic algorithms. For example, the overall process for solving the VVO problem is shown in Figure 2. To address the integer variables (i.e., the tap position of the OLTC and the number of shunt capacitors), in this paper, the local search method proposed in [35] was adopted, where the integer variables are relaxed to continuous variables and the two integer solutions closest to the relaxed-integer solution are then selected and compared.
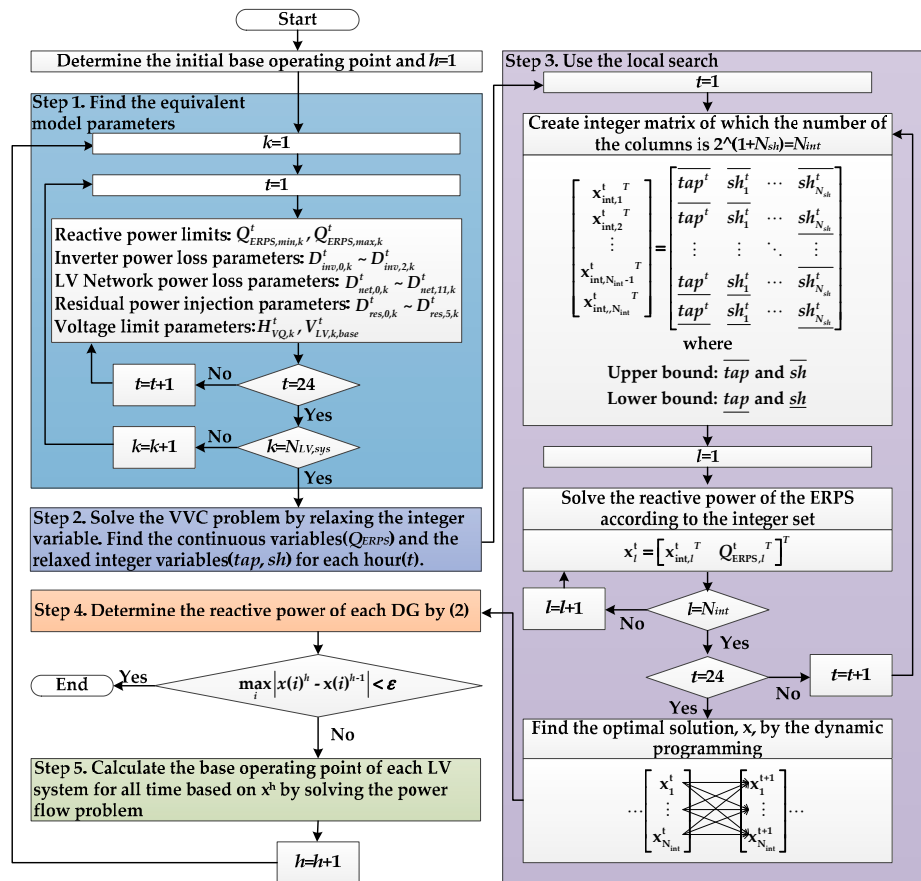
Start

Determine the initial base operating point and $h=1$

Step 1. Find the equivalent model parameters

$k=1$

$t=1$

Reactive power limits: $Q_{ERPS,min,k}^{t}$, $Q_{ERPS,max,k}^{t}$
Inverter power loss parameters: $D_{inv,0,k}^{t} \sim D_{inv,2,k}^{t}$
LV Network power loss parameters: $D_{net,0,k}^{t} \sim D_{net,11,k}^{t}$
Residual power injection parameters: $D_{res,0,k}^{t} \sim D_{res,5,k}^{t}$
Voltage limit parameters: $H_{VQ,k}^{t}$, $V_{LV,k,base}^{t}$

$t=t+1$　No　$t=24$　Yes

$k=k+1$　No　$k=N_{LV,sys}$　Yes

Step 2. Solve the VVC problem by relaxing the integer variable. Find the continuous variables(Q_{ERPS}) and the relaxed integer variables(tap, sh) for each hour(t).

Step 4. Determine the reactive power of each DG by (2)

End　Yes　$\max_{i} |x(i)^{h} - x(i)^{h-1}| < \varepsilon$　No

Step 5. Calculate the base operating point of each LV system for all time based on x^{h} by solving the power flow problem

$h=h+1$

Step 3. Use the local search

$t=1$

Create integer matrix of which the number of the columns is $2^{(1+N_{sh})}=N_{int}$

$$\begin{bmatrix} x_{int,1}^{t\ T} \\ x_{int,2}^{t\ T} \\ \vdots \\ x_{int,N_{int}-1}^{t\ T} \\ x_{int,N_{int}}^{t\ T} \end{bmatrix} = \begin{bmatrix} \overline{tap}^{t} & \overline{sh}_{1}^{t} & \cdots & \overline{sh}_{N_{sh}}^{t} \\ \overline{tap}^{t} & \underline{sh}_{1}^{t} & \cdots & \overline{sh}_{N_{sh}}^{t} \\ \vdots & \vdots & \ddots & \vdots \\ \underline{tap}^{t} & \overline{sh}_{1}^{t} & \cdots & \underline{sh}_{N_{sh}}^{t} \\ \underline{tap}^{t} & \underline{sh}_{1}^{t} & \cdots & \underline{sh}_{N_{sh}}^{t} \end{bmatrix}$$

where
Upper bound: $\overline{tap}$ and $\overline{sh}$
Lower bound: $\underline{tap}$ and $\underline{sh}$

$l=1$

Solve the reactive power of the ERPS according to the integer set

$$x_{l}^{t} = \begin{bmatrix} x_{int,l}^{t\ T} & Q_{ERPS,l}^{t\ T} \end{bmatrix}^{T}$$

$l=l+1$　No　$l=N_{int}$　Yes

$t=24$　No　$t=t+1$

Yes

Find the optimal solution, x, by the dynamic programming

$$\begin{bmatrix} x_{1}^{t} \\ \vdots \\ x_{N_{int}}^{t} \end{bmatrix} \quad \begin{bmatrix} x_{1}^{t+1} \\ \vdots \\ x_{N_{int}}^{t+1} \end{bmatrix}$$

Figure 2. Overall procedure for solving the proposed volt/var optimization (VVO) problem.

In Step 1, the parameters for the equivalent model of each LV system for all time are determined using the equations developed in Section 2; in Step 2, the VVO problem is relaxed to a nonlinear programing (NLP) problem and solved. In the relaxed solution, the tap position of the OLTC and the number of shunt capacitors are likely to be real values, rather than integer values; therefore, the local search is performed in Step 3, where the integer-solution sets are found to correctly represent the switching operations of the OLTC and the shunt capacitors. Consequently, the optimal solution for the *h*-th iteration, x^{h}, which consists of the tap position of the OLTC, the number of shunt capacitors, and the reactive power output of ERPS for all time, is determined in Step 3; in Step 4, based on the optimal value of Q_{ERPS}, the reactive power outputs of the individual DGs are determined using (2); after Step 4, the convergence is checked. If the variations in the decision variables are small enough, the iteration is terminated. Otherwise, a new base operating point of each LV system for all time is calculated by solving the power-flow problem based on x^{h} in Step 5. By updating the base operating point iteratively, the approximation errors of the proposed equivalent model can be reduced. In addition, the effect of the variation in inverter power loss on voltage magnitude is reflected on $V_{LV,k,base}^{t}$ in Equation (9).

Even though the active power profiles for the DGs and loads are fixed in the proposed method, the uncertainty of the DGs can be handled by using the proposed method to solve the VVO problem for each scenario of the scenario-based optimization methods [13–15]. If another method is used to solve the VVO problem, the proposed model can also be easily used by applying the parameter determination process, i.e., Steps 1, 4, and 5, into the original method, which corresponds to Steps 2 and 3, as shown in Figure 2.

4. Case Study

The accuracy of the proposed model for the LV system is validated using three different LV systems, particularly with respect to the power loss and residual power injection estimation. The VVO problem (19)–(28) is then solved to demonstrate the effectiveness of applying the proposed model to an optimal voltage control.

4.1. Accuracy of the Low-Voltage Power Loss Model

The test systems shown in Figure 3 were used to verify the proposed equivalent model. The active power outputs and the constants for the inverter power loss (i.e., $c_{inv,0,k,i}$, $c_{inv,1,k,i}$, and $c_{inv,2,k,i}$ in (3)) are summarized in Table 1. The rated capacities of all DGs were set to 6 kVA. The active and reactive power consumption values for each load were set to 10 kW and 8 kvar, respectively. The ZIP model coefficients of the loads are listed in Table 2 [29]. The impedances of the lines were $0.712 + j0.142 \ \Omega/\text{km}$, with line lengths of 25 m.
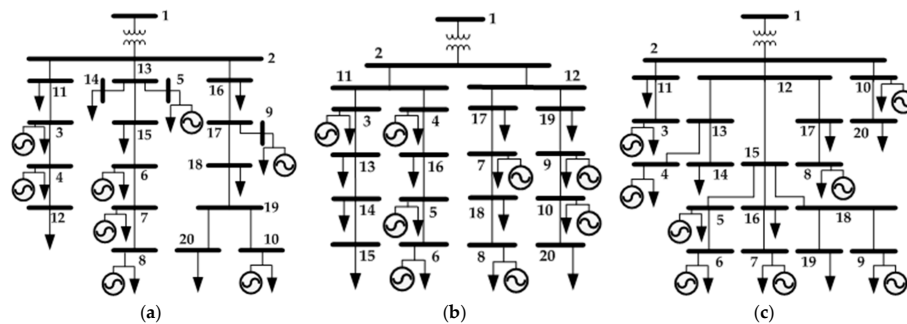

Figure 3. Three test low-voltage systems: 20 buses and 8 generators. (**a**) Low-voltage system 1; (**b**) low-voltage system 2; and (**c**) low-voltage system 3.

Table 1. Low-voltage system generation data and inverter power loss constants.

Bus No.	P_{DG} (kW)	$c_{inv,0}$	$c_{inv,1}$	$c_{inv,2}$
3	1.0	3.5×10^{-3}	5.0×10^{-3}	1.00×10^{-2}
4	1.6	3.5×10^{-3}	5.0×10^{-3}	1.00×10^{-2}
5	2.2	3.7×10^{-3}	5.2×10^{-3}	1.05×10^{-2}
6	2.8	3.7×10^{-3}	5.2×10^{-3}	1.05×10^{-2}
7	3.4	3.9×10^{-3}	5.4×10^{-3}	1.1×10^{-2}
8	4.0	3.9×10^{-3}	5.4×10^{-3}	1.1×10^{-2}
9	4.6	4.1×10^{-3}	5.6×10^{-3}	1.15×10^{-2}
10	5.2	4.1×10^{-3}	5.6×10^{-3}	1.15×10^{-2}

Table 2. Constant impedance-current-power (ZIP) model parameters.

Type	$K_{P,2}$	$K_{P,1}$	$K_{P,0}$	$K_{Q,2}$	$K_{Q,1}$	$K_{Q,0}$
1 [1]	1.21	−1.61	1.4	4.35	−7.08	3.73
2 [2]	1.5	−2.31	1.81	7.41	−11.97	5.56
3 [3]	0.4	−0.41	1.01	4.43	−7.98	4.55

[1] Bus 3~8, [2] Bus 9~14, and [3] Bus 15~ 20.

The network power loss estimated using (15) and the residual power injection calculated using (18) were compared with those calculated using general power-flow equations with the detailed network model, with the voltage magnitude of Bus 1 being changed from 0.95 p.u. to 1.05 p.u., and the reactive power output of the ERPS being changed from −38.8 kvar to 38.8 kvar. The reactive power outputs of the individual DGs were determined using (2). The base operating point is derived when Q_{ERPS} = 0 kvar and V_{MV} = 1 p.u. Figure 4 shows the errors of the network power loss and residual power injection for LV system 1. The results for LV systems 2 and 3 were similar to those shown in Figure 4, and are presented in Appendix D. The maximum network power loss error and the residual power injection error for all of the LV systems were less than 2.89% and 0.13%, respectively. A large change in the network operating point can increase the error in the result, as shown in Figure 4. However, it does not degrade the accuracy of the VVO, as demonstrated in Section 4.2, because the base operating point is actively adjusted during the process of solving the VVO problem, as shown in Figure 2. For the total inverter power loss of the LV system, the results obtained using the proposed model were compared to the sum of the individual inverter power losses calculated using (3), which was given in [25,26]. As shown in Figure 5, the maximum difference was less than 0.78%.
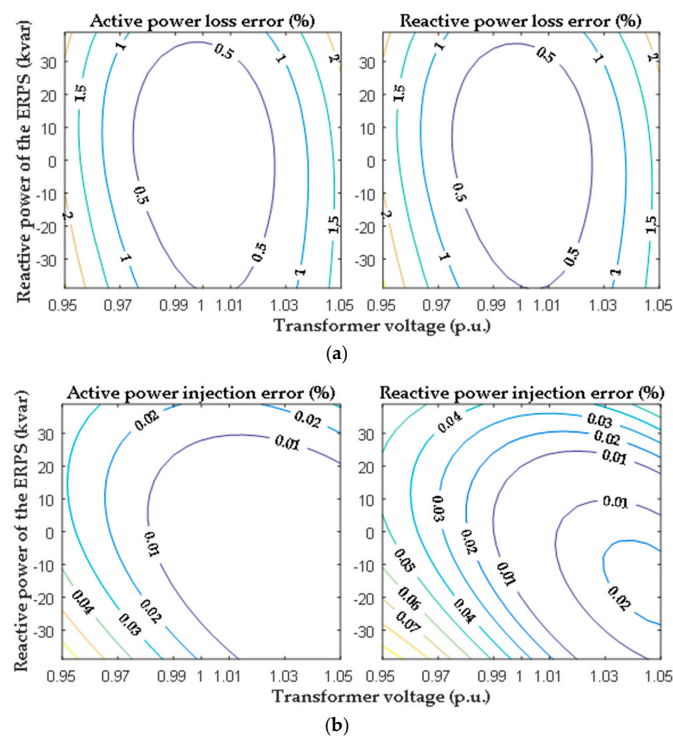

Figure 4. Error in the network power loss and residual power injection for low-voltage system 1. (**a**) Network power loss; (**b**) Residual power injection.
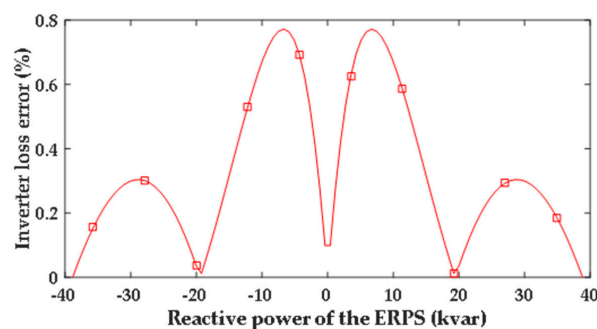

Figure 5. Error in the inverter power loss model.

4.2. Effect on the Volt/Var Optimization

The VVO program was developed using MATLAB from the MathWorks, Inc. (Natick, MA, USA) and the interior point method, which is widely used to solve the NLP problem. The simulations were performed using a PC with an Intel Core i7-4770K 3.5 GHz processor and 16 GB of memory. The modified Institute of electrical and electronics engineers (IEEE) 13-node test feeder shown in Figure 6 was used to analyze the advantages of applying the proposed model to the VVO. The OLTC is located between Bus 650 and Bus 632 to regulate the feeder voltage from −10% to 10% in 32 steps. Two 100 kvar capacitors were connected to Bus 675 in three phases, and one 100 kvar capacitor was connected to Bus 684 in phases A and C. Twelve LV systems, with network topologies and line parameters specified in Section 4.1, were connected to MV Buses 633, 646, 671, 680, 652, and 611.
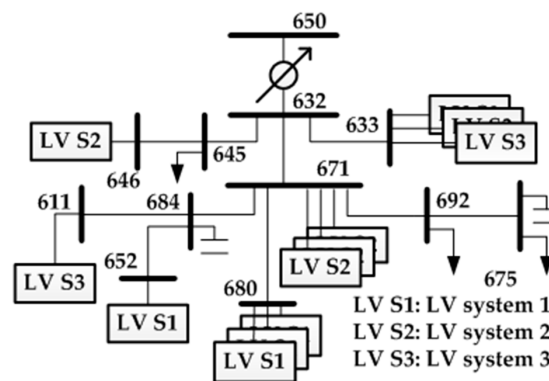

Figure 6. Modified Institute of electrical and electronics engineers (IEEE) 13-bus test feeder.

Figure 7 shows the three types of load-demand profile that were considered, representing industrial, residential, and commercial load demands. The profile represents the ratio of the load demand to the average load demand presented in Table 3. The coefficients of the ZIP model for industrial, residential, and commercial loads are equal to those of types 1, 2, and 3 listed in Table 2, respectively. The active power profile of the DG corresponds to one of the three previously dispatched profiles shown in Figure 8. The DGs connected to the same LV system have the same rated capacities as well as the same inverter power loss constants. Table 4 shows the generation pattern types, the capacities, and the inverter power loss constants of the DGs. For the objective function (19), the cost weights w_P, w_{tap}, and w_{sh} were set to 0.03, 0.12, and 0.05, respectively. The minimum and maximum voltage limits for the MV and LV distribution systems were 0.95 p.u. and 1.05 p.u., respectively.
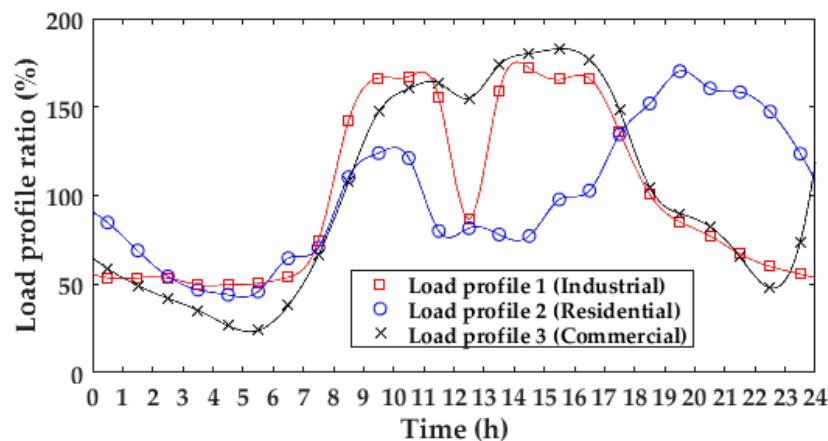

Figure 7. Three different load-demand profiles for industrial, residential, and commercial loads.

Table 3. Average load demand.

Bus No.	Phase	Active Power, $P_{L,norm}$ (kW)	Reactive Power, $Q_{L,norm}$ (kvar)	Load Profile
	A	105 (7.5 *)	61 (4.4 *)	1
633	B	69 (4.9 *)	40 (2.9 *)	1
	C	69 (4.9 *)	40 (2.9 *)	1
645	B	131	76	2
646	B	119 (7.4 *)	69 (4.3 *)	2
	A	99 (6.2 *)	57 (3.6 *)	2
671	B	99 (6.2 *)	57 (3.6 *)	2
	C	99 (6.2 *)	57 (3.6 *)	2
	A	65	38	3
692	B	65	38	3
	C	65	38	3
	A	174	101	1
675	B	131	76	1
	C	184	107	1
	A	99 (6.6 *)	57 (3.8 *)	3
680	B	111 (7.4 *)	64 (4.3 *)	3
	C	105 (7.0 *)	61 (4.1 *)	3
684	A	65	38	1
	C	65	38	1
652	A	73 (4.9 *)	42 (2.8 *)	2
611	C	86 (6.1 *)	50 (3.6 *)	2

* Values in parentheses represent the load demand on each bus in the LV system.
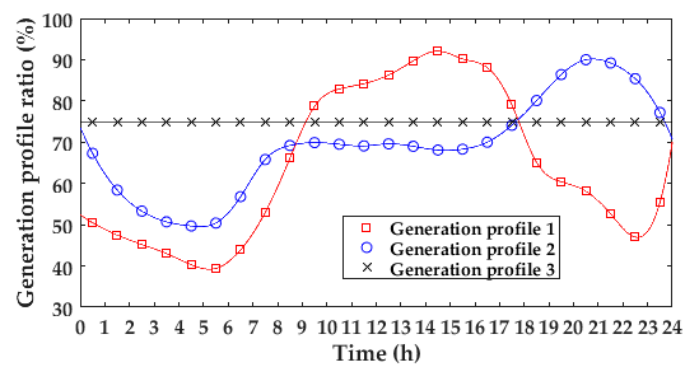
Figure 8. Three different profiles for the dispatched active power of the distributed generator (DG).

Table 4. Detailed DG specifications.

Bus No.	DG Capacity *	Generation Profile
652, 680	120%	1
671, 646	80%	2
633, 611	40%	3
Inverter power loss constants	$c_{inv,0}$　$c_{inv,1}$	$c_{inv,2}$
	3.5×10^{-3}　5.0×10^{-3}	1.00×10^{-2}

* The percentage means the ratio of the maximum capacity of the DG to the average load demand.

The results of the following three cases were then compared to evaluate the effects of the application of the proposed model on the VVO.

- Case 1: The DGs in the LV systems are not utilized for the VVO. Detailed models of the LV systems are used in the VVO.

- Case 2: The DGs in the LV systems are utilized for the VVO. Detailed models of the LV systems are used in the VVO. In other words, the reactive power outputs of the DGs are determined by solving a detailed optimal power flow problem, not by using Equation (2).
- Case 3: The DGs in the LV systems are utilized for the VVO. However, the proposed model is used in the VVO.

In Case 3, the initial base operating points of all LV systems are determined under conditions where the voltage magnitudes of the MV buses and the reactive power outputs of all DGs are set to 1.0 p.u. and 0 kvar, respectively.

The results for the cases are summarized in Table 5. The total active power loss and the number of switching operations in Case 2 were less than those in Case 1. This demonstrated that the VVO scheme considering the DGs in the LV systems effectively reduces the power losses in the MV and LV systems as well as the number of switching operations in the MV system. However, the computational time required to solve the VVO problem increased, as shown in Figure 9, owing to the increase in the number of decision variables (i.e., the reactive power reference for the DGs for the optimization problem). On the other hand, by using the proposed model (i.e., Case 3), the computational time was notably decreased, while the VVO results were almost identical to those obtained using the detailed model (i.e., Case 2). This is because the size of the NLP problem is significantly reduced by replacing the LV system with the proposed model, as shown in Figure 9, and thus the computational time required for Steps 2 and 3 shown in Figure 2 is decreased.

Table 5. Case study results for different VVO methods.

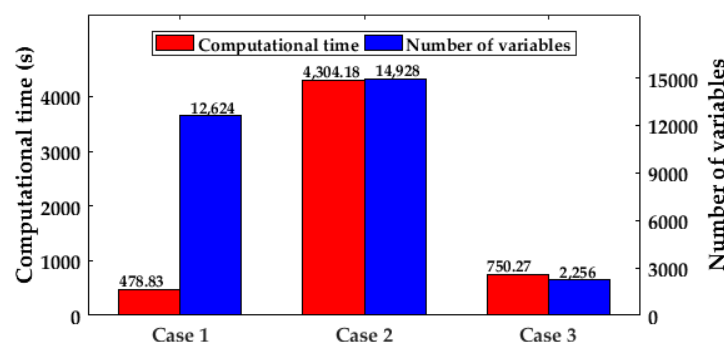| Parameters		Case 1	Case 2	Case 3
MV network active power loss (kWh)		340	319	319
LV network active power loss (kWh)		915	744	745
Inverter active power loss (kWh)		137	174	175
Total active power loss (kWh)		1392	1237	1239
Number of OLTC operations		8	2	2
Number of shunt capacitor operations	675A	4	2	2
	675B	0	2	2
	675C	2	2	2
	684A	2	0	0
	684C	2	0	0
Total number of switching operations		18	8	8

Figure 9. Computational time and number of variables.

5. Conclusions

In this paper, a new analytical equivalent model for an LV distribution system that accommodates inverter-based DGs was proposed considering the effects of the reactive power control of the DGs on the power losses, voltage magnitudes, and power consumption of loads in the LV system. The proposed equivalent model consists mainly of an ERPS that corresponds to the controllable reactive

power source, as well as the LV power loss component, which indicates the effect of the DG reactive power control on the network power loss and the inverter power loss. In addition, a method to apply the proposed model to a VVO problem, which considers not only MV systems but also LV systems, was proposed. Because the proposed model was developed using analytic equations, it can be applied to the VVO using the deterministic-optimization method with few modifications. In the case study, it was verified that by using the proposed model, the computational time required to solve the VVO problem can be reduced significantly without degradation of the accuracy of the optimal solution.

Author Contributions: Mu-Gu Jeong proposed the main idea and wrote the paper. Young-Jin Kim checked the overall logic of this work and revised the paper. Seung-Il Moon designed the case studies. Pyeong-Ik Hwang supervised this work and revised the paper.

Conflicts of Interest: The authors declare no conflict of interest.

Nomenclature

Matrices and vectors are denoted using bold letters, e.g., $x_{m,i}$ is the *m*-th row and *i*-th column element of **x**.

Indices and subscripts

k, n	Indices of the MV buses
i, m	Indices of the LV buses
l	Index of the integer variables
β	Index of the impedance-current-power (ZIP) coefficient
t	Index of the hours *
h	Index of the iterations *
base	Subscript for the base operating point
min, max	Subscripts for the minimum and maximum limits

Variables

$E_{MV(LV)}$, $\theta_{MV(LV)}$, $V_{MV(LV)}$	Voltage phasor, magnitude, and angle of each MV (LV) bus
$P_{MV(LV)}$, $Q_{MV(LV)}$, $S_{MV(LV)}$	Active, reactive, and complex power injection into each MV (LV) bus
P_{DG}, Q_{DG}, S_{DG}	Active, reactive, and complex power of each DG
$P_{DG,inv}$	Actual active power of each DG excluding the inverter power loss
S_{rated}	Rated capacity of the inverter of each DG
P_{Load}, Q_{Load}	Active and reactive power of each load
$P_{L,norm}$, $Q_{L,norm}$	Active and reactive power of each load when voltage = 1 p.u.
K_P, K_Q	ZIP coefficients for active and reactive powers
$I_{MV(LV)}$	Injection current into each MV (LV) bus
Y_1	Self-admittance of an MV bus connected to an LV system
Y_2	Admittance between the MV bus and an LV system
Y_3	Admittance of an LV system
G_{MV}, B_{MV}	Conductance and susceptance of the MV system
Q_{ERPS}	Aggregated reactive power of the DGs in an LV system
α	Ratio of Q_{DG} to Q_{ERPS}
$P_{inv,loss}$	Aggregated inverter power loss of the DGs in an LV system
$P_{net,loss}$, $Q_{net,loss}$, $S_{net,loss}$	Network active, reactive, and complex losses in an LV system
P_{res}, Q_{res}	Residual active and reactive power injections in an LV system
tap	Tap position
sh	Number of unit capacitors connected to the MV feeders
w_P, w_{tap}, w_{sh}	Cost weights of the objective function
H_{VQ}	Voltage sensitivity with respect to the reactive powers of the ERPS
W_{VQ}	Voltage sensitivity matrix with respect to the individual reactive powers of the DGs in an LV system
N_{sh}	Total number of shunt capacitors in an MV system
$N_{LV,sys}$	Total number of LV systems in an MV system
$N_{MV,Bus}$	Total number of MV buses
$N_{LV,Bus}$	Total number of buses in the LV system connected to an MV bus
$N_{LV,DG}$	Total number of DGs in the LV system connected to an MV bus

<div align="center">* Superscript index.</div>

Appendix A. Inverter Power Loss

Using a quadratic Lagrange polynomial with three interpolation points that correspond to the maximum, half, and none of the DG reactive power outputs, (3) can be interpolated as:

$$P_{inv,loss,k,i}^{t} = d_{inv,1,k,i}\left|Q_{DG,k,i}^{t}\right| + d_{inv,2,k,i}\left(Q_{DG,k,i}^{t}\right)^{2} + \Gamma_{inv,k,i}^{t}, \tag{A1}$$

where:

$$d_{inv,1,k,i} = \frac{4f_{inv,loss,k,i}\left(Q_{DG,\max,k,i}^{t}/2\right) - f_{inv,loss,k,i}\left(Q_{DG,\max,k,i}^{t}\right)}{Q_{DG,\max,k,i}^{t}},$$

$$d_{inv,2,k,i} = \frac{2f_{inv,loss,k,i}\left(Q_{DG,\max,k,i}^{t}\right) - 4f_{inv,loss,k,i}\left(Q_{DG,\max,k,i}^{t}/2\right)}{\left(Q_{DG,\max,k,i}^{t}\right)^{2}},$$

$$\Gamma_{inv,k,i}^{t} = c_{inv,0,k,i}S_{rated,i} + c_{inv,1,k,i}P_{DG,k,i}^{t} + \frac{c_{inv,2,k,i}}{S_{rated,k,i}}\left(P_{DG,k,i}^{t}\right)^{2},$$

$$f_{inv,loss,k,i}(x) = c_{inv,1,k,i}\left(\sqrt{P_{DG,k,i}^{t}{}^{2} + x^{2}} - P_{DG,k,i}^{t}\right) + \frac{c_{inv,2,k,i}}{S_{rated,k,i}}x^{2}.$$

By substituting (2) into (A1) and summing all the inverter power losses of the DGs, the total inverter power loss in the LV system is formulated as (4), where:

$$D_{inv,0,k}^{t} = \sum_{i=1}^{N_{LV,DG,k}} \Gamma_{inv,k,i}^{t}, D_{inv,1,k}^{t} = \sum_{i=1}^{N_{LV,DG,k}} d_{inv,1,k,i}\alpha_{k,i}^{t}, D_{inv,2,k}^{t} = \sum_{i=1}^{N_{LV,DG,k}} d_{inv,2,k,i}\left(\alpha_{k,i}^{t}\right)^{2}.$$

Appendix B. Voltage Magnitude Variations in the Low-Voltage System

The matrix of the voltage magnitude sensitivity to the reactive power outputs of the DGs can be derived as:

$$\mathbf{W_{VQ,k,base}^{t}} = \left(\mathbf{J_{LV,QV,k,base}^{t}} - \mathbf{J_{LV,Q\theta,k,base}^{t}}\mathbf{J_{LV,P\theta,k,base}^{t}}^{-1}\mathbf{J_{LV,PV,k,base}^{t}}\right)^{-1}, \tag{A2}$$

where the Jacobian matrix of the LV system is shown as:

$$\begin{bmatrix} \Delta\mathbf{P_{LV,k}^{t}} \\ \Delta\mathbf{Q_{LV,k}^{t}} \end{bmatrix} = \begin{bmatrix} \mathbf{J_{LV,P\theta,k}^{t}} & \mathbf{J_{LV,PV,k}^{t}} \\ \mathbf{J_{LV,Q\theta,k}^{t}} & \mathbf{J_{LV,QV,k}^{t}} \end{bmatrix} \begin{bmatrix} \Delta\boldsymbol{\theta_{LV,k}^{t}} \\ \Delta\mathbf{V_{LV,k}^{t}} \end{bmatrix}.$$

Based on (A2), the voltage magnitude variation on the *i*-th bus, resulting from the reactive power control of the ERPS, is obtained as:

$$\Delta V_{LV,1,k,i}^{t} = \sum_{m=1}^{N_{LV,DG,k}} W_{VQ,k,i,m,base}^{t}\alpha_{k,m}^{t}Q_{ERPS,k}^{t} - \sum_{m=1}^{N_{LV,DG,k}} W_{VQ,k,i,m,base}^{t}\alpha_{k,m}^{t}Q_{ERPS,k,base}^{t} = H_{VQ,k,i}^{t}\left(Q_{ERPS,k}^{t} - Q_{ERPS,k,base}^{t}\right). \tag{A3}$$

Meanwhile, the voltage magnitude variation of MV bus *k* has almost the same effect on the voltage magnitudes of the buses in the LV system [30], i.e., (A4):

$$\Delta V_{LV,2,k,i}^{t} \approx \Delta V_{MV,k}^{t} = V_{MV,k}^{t} - V_{MV,k,base}^{t}. \tag{A4}$$

By adding (A3) and (A4), the total variation in the voltage magnitude is then given as (A5):

$$\Delta V_{LV,k,i}^{t} \approx H_{VQ,k,i}^{t}\left(Q_{ERPS,k}^{t} - Q_{ERPS,k,base}^{t}\right) + V_{MV,k}^{t} - V_{MV,k,base}^{t}, \tag{A5}$$

which supports (9).

Appendix C. Network Power Loss

Using (11) and (12), (13) is expressed as:

$$
S^t_{net.loss,k} = C_{VV,k}{}^* V^t_{MV,k}{}^2 + E^t_{MV,k} \sum_{i=1}^{N_{LV,Bus,k}} C_{VI,k,i} I^t_{LV,k,i}{}^* + \sum_{i=1}^{N_{LV,Bus,k}} \sum_{m=1}^{N_{LV,Bus,k}} C_{II,k,i,m} I^t_{LV,k,m} I^t_{LV,k,i}{}^*, \tag{A6}
$$

where $C_{VI,k,i} = \left(\sum\limits_{m=1}^{N_{LV,Bus,k}} Y_{2,k,m}{}^* C_{II,k,m,i}{}^* - \sum\limits_{m=1}^{N_{LV,Bus,k}} C_{II,k,i,m} Y_{2,k,m} \right)$.

Then, using $I^* = S/E = (S/V)\angle(-\theta)$, (A6) is modified to:

$$
\begin{aligned}
S^t_{net.loss,k} &= C_{VV,k}{}^* V^t_{MV,k}{}^2 + V^t_{MV,k} \sum_{i=1}^{N_{LV,Bus,k}} C_{VI,k,i} \left(\frac{S^t_{LV,k,i}}{V^t_{LV,k,i}} \right) \angle \left(\theta^t_{MV,k} - \theta^t_{LV,k,i} \right) \\
&+ \sum_{i=1}^{N_{LV,Bus,k}} \sum_{m=1}^{N_{LV,Bus,k}} C_{II,k,i,m} \left(\frac{S^t_{LV,k,i}}{V^t_{LV,k,i}} \right) \left(\frac{S^t_{LV,k,m}}{V^t_{LV,k,m}}{}^* \right) \angle \left(\theta^t_{LV,k,m} - \theta^t_{LV,k,i} \right)
\end{aligned} \tag{A7}
$$

Because the angle difference is reasonably small under normal operating conditions [31,32], (A7) is approximated to (14) by neglecting the angle difference. S/V in (14) is expressed as:

$$
\frac{S^t_{LV,k,i}}{V^t_{LV,k,i}} = \frac{P^t_{DG,inv,k,i,base} - \sum\limits_{\beta=0}^{2} P^t_{L,norm,k,i} K^t_{P,k,i,\beta} V^t_{LV,k,i}{}^{\beta}}{V^t_{LV,k,i}} + j \frac{\alpha^t_{k,i} Q^t_{ERPS,k} - \sum\limits_{\beta=0}^{2} Q^t_{L,norm,k,i} K^t_{Q,k,i,\beta} V^t_{LV,k,i}{}^{\beta}}{V^t_{LV,k,i}}. \tag{A8}
$$

On the other hand, the voltage magnitude deviation in (A5) is considerably small under normal conditions because the voltage magnitude is maintained within operational bounds by a VVO. Considering the first term of the Taylor series, the fractional expressions in (A8) are approximated to:

$$
\frac{P^t_{DG,inv,k,i,base}}{V^t_{LV,k,i}} \approx \frac{P^t_{DG,inv,k,i,base}}{V^t_{LV,k,i,base}} - \frac{P^t_{DG,inv,k,i,base}}{V^t_{LV,k,i,base}{}^2} \Delta V^t_{LV,k,i}, \tag{A9}
$$

$$
\frac{\alpha^t_{k,i} Q^t_{ERPS,k}}{V^t_{LV,k,i}} \approx \frac{\alpha^t_{k,i} Q^t_{ERPS,k}}{V^t_{LV,k,i,base}} - \frac{\alpha^t_{k,i} Q^t_{ERPS,k}}{V^t_{LV,k,i,base}{}^2} \Delta V^t_{LV,k,i}, \tag{A10}
$$

$$
\begin{aligned}
& \sum_{\beta=0}^{2} P^t_{L,norm,k,i} K^t_{P,k,i,\beta} V^t_{LV,k,i}{}^{\beta-1} \\
&\approx \sum_{\beta=0}^{2} P^t_{L,norm,k,i} K^t_{P,k,i,\beta} V^t_{LV,k,i,base}{}^{\beta-1} - \sum_{\beta=0}^{2} (\beta-1) P^t_{L,norm,k,i} K^t_{P,k,i,\beta} V^t_{LV,k,i,base}{}^{\beta-2} \Delta V^t_{LV,k,i}
\end{aligned} \tag{A11}
$$

$$
\begin{aligned}
& \sum_{\beta=0}^{2} Q^t_{L,norm,k,i} K^t_{Q,k,i,\beta} V^t_{LV,k,i}{}^{\beta-1} \\
&\approx \sum_{\beta=0}^{2} Q^t_{L,norm,k,i} K^t_{Q,k,i,\beta} V^t_{LV,k,i,base}{}^{\beta-1} - \sum_{\beta=0}^{2} (\beta-1) Q^t_{L,norm,k,i} K^t_{Q,k,i,\beta} V^t_{LV,k,i,base}{}^{\beta-2} \Delta V^t_{LV,k,i}
\end{aligned} \tag{A12}
$$

Using (A5), (A9)–(A12), (A8) is approximated as:

$$
\frac{S^t_{LV,k,i}}{V^t_{LV,k,i}} \approx d^t_{net,0,k,i} + d^t_{net,1,k,i} Q^t_{ERPS,k} + d^t_{net,2,k,i} Q^t_{ERPS,k}{}^2 + \left(d^t_{net,3,k,i} + d^t_{net,4,k,i} Q^t_{ERPS,k} \right) V^t_{MV,k}, \tag{A13}
$$

where:

$$
d^t_{net,0,k,i} = \frac{P^t_{DG,inv,k,i,base}}{V^t_{LV,k,i,base}} - \frac{P^t_{DG,inv,k,i,base}}{V^t_{LV,k,i,base}{}^2} c_{net,0,k,i} - c_{net,1,k,i} - c_{net,2,k,i} c_{net,0,k,i},
$$

$$
d^t_{net,1,k,i} = -\frac{P^t_{DG,inv,k,i,base} H^t_{VQ,k,i}}{V^t_{LV,k,i,base}{}^2} + j \frac{\alpha^t_{k,i}}{V^t_{LV,k,i,base}} - j \frac{\alpha^t_{k,i} c_{net,0,k,i}}{V^t_{LV,k,i,base}{}^2} - c_{net,2,k,i} H^t_{VQ,k,i}, d^t_{net,2,k,i} = -j \frac{\alpha^t_{k,i} H^t_{VQ,k,i}}{V^t_{LV,k,i,base}{}^2},
$$

$$
d^t_{net,3,k,i} = -\frac{P^t_{DG,inv,k,i,base}}{V^t_{LV,k,i,base}{}^2} - c_{net,2,k,i}, d^t_{net,4,k,i} = -j \frac{\alpha^t_{k,i}}{V^t_{LV,k,i,base}{}^2}, c_{net,0,k,i} = -H^t_{VQ,k,i} Q^t_{ERPS,k,base} - V^t_{MV,k,base},
$$

$$c_{net,1,k,i} = \sum_{\beta=0}^{2} P_{L,norm,k,i}^{t} K_{P,k,i,\beta}^{t} V_{LV,k,i,base}^{t}{}^{\beta-1} + j \sum_{\beta=0}^{2} Q_{L,norm,k,i}^{t} K_{Q,k,i,\beta}^{t} V_{LV,k,i,base}^{t}{}^{\beta-1},$$

$$c_{net,2,k,i} = \sum_{\beta=0}^{2} (\beta-1) P_{L,norm,k,i}^{t} K_{P,k,i,\beta}^{t} V_{LV,k,i,base}^{t}{}^{\beta-2} + j \sum_{\beta=0}^{2} (\beta-1) Q_{L,norm,k,i}^{t} K_{Q,k,i,\beta}^{t} V_{LV,k,i,base}^{t}{}^{\beta-2},$$

By substituting (A13) into (14), (14) is expressed as (15), where:

$$D_{net,0,k}^{t} = e_{a,0,k}^{t}, D_{net,1,k}^{t} = e_{b,1,0,k}^{t}, \ D_{net,2,k}^{t} = e_{a,1,k}^{t} + e_{b,2,0,k}^{t}, \ D_{net,3,k}^{t} = e_{b,2,1,k}^{t}, \ D_{net,4,k}^{t} = e_{a,2,k}^{t},$$

$$D_{net,5,k}^{t} = e_{b,3,0,k}^{t} + e_{c,0,k}^{t}, \ D_{net,6,k}^{t} = e_{b,3,1,k}^{t} + e_{b,4,0,k}^{t} + e_{c,1,k}^{t}, \ D_{net,7,k}^{t} = e_{b,3,2,k}^{t} + e_{b,4,1,k}^{t} + e_{c,2,k}^{t}, \ D_{net,8,k}^{t} = e_{b,4,2,k}^{t},$$

$$D_{net,9,k}^{t} = C_{VV,k}{}^{*} + e_{a,3,k}^{t} + e_{c,3,k}^{t}, \ D_{net,10,k}^{t} = e_{b,4,3,k}^{t} + e_{c,4,k}^{t}, \ D_{net,11,k}^{t} = e_{a,4,k}^{t},$$

$$e_{a,M,k}^{t} = \sum_{i=1}^{N_{LV,Bus,k}} \sum_{m=1}^{N_{LV,Bus,k}} C_{II,k,i,m} d_{net,M,k,i}^{t} d_{net,M,k,i}^{t}{}^{*}, e_{b,J,M,k}^{t} = 2 \sum_{i=1}^{N_{LV,Bus,k}} \sum_{m=1}^{N_{LV,Bus,k}} C_{II,k,i,m} \mathrm{Re}\left\{ d_{net,J,k,i}^{t} d_{net,M,k,i}^{t}{}^{*} \right\},$$

$$e_{c,M,k}^{t} = \sum_{i=1}^{N_{LV,Bus,k}} C_{VI,k,i} d_{net,M,k,i}^{t}.$$

Appendix D. Equivalent Model Error in Low-Voltage Systems 2 and 3

The errors in the network power losses and residual power injections for LV systems 2 and 3 are illustrated in Figures A1 and A2,
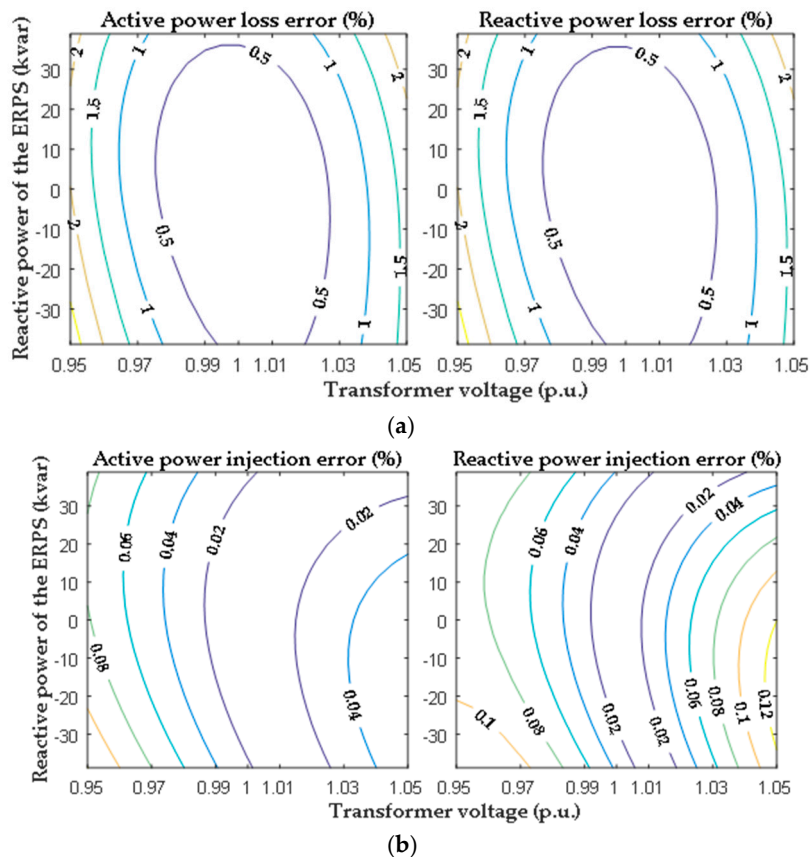

(a)

(b)

Figure A1. Error in the network power loss and residual power injection for low-voltage system 2. (**a**) Network power loss; and (**b**) residual power injection.
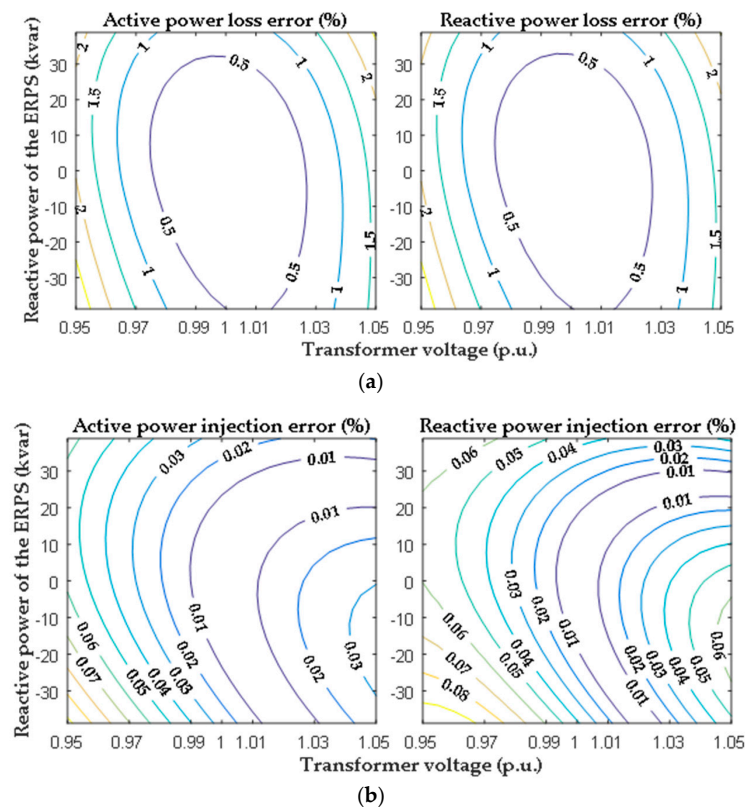
Figure A2. Error in the network power loss and residual power injection for low-voltage system 3. (a) Network power loss; and (b) residual power injection.

References

1. Chiradeja, P.; Ramakumar, R. An approach to quantify the technical benefits of distributed generation. *IEEE Trans. Energy Convers.* **2004**, *19*, 764–773. [CrossRef]

2. Keane, A.; Ochoa, L.F.; Vittal, E.; Dent, C.J.; Harrixon, G.P. Enhanced utilization of voltage control resources with distributed generation. *IEEE Trans. Power Syst.* **2011**, *26*, 252–260. [CrossRef]

3. Carvalho, P.M.S.; Correia, P.F.; Ferreira, L.A.F.M. Distributed reactive power generation control for voltage rise mitigation in distribution networks. *IEEE Trans. Power Syst.* **2008**, *23*, 766–772. [CrossRef]

4. Mohapatra, A.; Bijwe, P.R.; Panigrahi, B.K. An efficient hybrid approach for volt/var control in distribution systems. *IEEE Trans. Power Deliv.* **2014**, *29*, 1780–1788. [CrossRef]

5. Kim, Y.J.; Ahn, S.J.; Hwang, P.I.; Pyo, G.C.; Moon, S.I. Coordinated control of a DG and voltage control devices using a dynamic programming algorithm. *IEEE Trans. Power Syst.* **2013**, *28*, 42–51. [CrossRef]

6. Samimi, A.; Kazemi, A. A new approach to optimal allocation of reactive power ancillary service in distribution systems in the presence of distributed energy resources. *Appl. Sci.* **2015**, *5*, 1284–1309. [CrossRef]

7. Hwang, P.I.; Moon, S.I.; Ahn, S.J. A conservation voltage reduction scheme for a distribution systems with intermittent distributed generators. *Energies* **2016**, *9*, 666. [CrossRef]

8. Von Appen, J.; Braun, M.; Stetz, T.; Diwold, K.; Geibel, D. Time in the Sum: the challenge of high PV penetration in the German electric grid. *IEEE Power Energy Mag.* **2013**, *11*, 55–64. [CrossRef]

9. Thomson, M.; Infield, D.G. Network power-flow analysis for a high penetration of distributed generation. *IEEE Trans. Power Syst.* **2007**, *22*, 1157–1162. [CrossRef]

10. Trichakis, P.; Taylor, P.C.; Lyons, P.F.; Hair, R. Predicting the technical impacts of high level of small-scale embedded generators on low-voltage networks. *IET Renew. Power Gener.* **2008**, *2*, 249–262. [CrossRef]

11. Braun, M.; Stetz, T.; Brundlinger, R.; Mayr, C.; Ogimoto, K.; Hatta, H.; Kobayashi, H.; Kroposki, B.; Mather, B.; Coddington, M.; et al. Is the distribution grid ready to accept large-scale photovoltaic deployment? State of art, progress, and future prospects. *Prog. Photovolt.* **2012**, *20*, 681–697. [CrossRef]

12. Samadi, A.; Eriksson, R.; Soder, L.; Rawn, B.G.; Boemer, J.C. Coordinated active power dependent voltage regulation in distribution grids with PV systems. *IEEE Trans. Power Deliv.* **2014**, *29*, 1454–1464. [CrossRef]

13. Niknam, T.; Zare, M.; Aghaei, J. Scenario-based multiobjective volt/var control in distribution networks including renewable energy sources. *IEEE Trans. Power Deliv.* **2012**, *27*, 2004–2019. [CrossRef]

14. Wang, Z.; Wang, J.; Chen, B.; Begovic, M.M.; He, Y. MPC-based voltage/var optimization for distribution circuits with distributed generators and exponential load models. *IEEE Trans. Smart Grid* **2014**, *5*, 2412–2420. [CrossRef]

15. Zhang, C.; Chen, H.; Ngan, H. Reactive power optimisation considering wind farms based on an optimal scenario method. *IET Gener. Trans. Distrib.* **2016**, *10*, 3736–3744. [CrossRef]

16. Ward, J.B. Equivalent circuits for power flow studies. *AIEE Trans.* **1949**, *68*, 373–382. [CrossRef]

17. Liacco, T.E.D.; Savulescu, S.C.; Ramaro, K.A. An on-line topological equivalent of a power system. *IEEE Trans. Power Appar. Syst.* **1978**, *PAS-97*, 1550–1563. [CrossRef]

18. Collin, A.J.; Acosta, J.L.; Hernando-Gil, I.; Djokic, S.Z. An 11kV steady state residential aggregate load model. Part 2: Microgeneration and demand-side management. In Proceedings of the 2011 IEEE Trondheim PowerTech, Trondheim, Norway, 19–23 June 2011.

19. Collin, A.J.; Tsagarakis, G.; Kiprakis, A.E.; McLaughlin, S. Development of low-voltage load models for the residential load sector. *IEEE Trans. Power Syst.* **2014**, *29*, 2180–2188. [CrossRef]

20. Di Fazio, A.R.; Russo, M.; Valeri, S.; De Santis, M. Sensitivity-based model of low voltage distribution systems with distributed energy resources. *Energies* **2016**, *9*, 801. [CrossRef]

21. Samadi, A.; Soder, L.; Shayestech, E.; Eriksson, R. Static equivalent of distribution grids with high penetration of PV systems. *IEEE Trans. Smart Grid* **2015**, *6*, 1763–1774. [CrossRef]

22. Madureira, A.G.; Lopes, J.A.P. Coordinated voltage support in distribution networks with distributed generation and microgrids. *IET Renew. Power Gener.* **2009**, *3*, 439–454. [CrossRef]

23. Hemmati, R.; Hooshmand, R.A.; Khodabakhshian, A. State-of-the-art of transmission expansion planning: Comprehensive review. *Renew. Sustain. Energy Rev.* **2013**, *23*, 312–319. [CrossRef]

24. Su, X.; Masoum, M.A.S.; Wolfs, P.J. Optimal PV inverter reactive power control and real power curtailment to improve performance of unbalanced four-wire LV distribution networks. *IEEE Trans. Sustain. Energy* **2014**, *5*, 967–977. [CrossRef]

25. Braun, M. Reactive power supplied by PV inverters-cost benefit analysis. In Proceedings of the 22nd European Photovoltaic Solar Energy Conference and Exhibition, Milan, Italy, 3–7 September 2007.

26. El-Aal, M.A.A. Modelling and Simulation of a Photovoltaic Fuel Cell Hybrid System. Ph.D. Thesis, University of Kassel, Kassel, Germany, 2005.

27. Chapra, S.C.; Canale, R.P. *Numerical Methods for Engineers*, 6th ed.; McGraw-Hill: Boston, MA, USA, 2011; pp. 500–501.

28. Kundur, P. *Power System Stability and Control*; McGraw-Hill: New York, NY, USA, 1994; p. 273.

29. Bokhari, A.; Alkan, A.; Dogan, R.; Auilo, M.D.; Leon, F.; Czarkowski, D.; Zabar, Z.; Birenbaum, L.; Noel, A.; Uosef, R.E. Experimental determination of the ZIP coefficients for modern residential, commercial, and industrial loads. *IEEE Trans. Power Deliv.* **2014**, *29*, 1372–1381. [CrossRef]

30. Azzouz, M.A.; Farag, H.E.; El-Saadany, E.F. Real-time fuzzy voltage regulation for distribution networks incorporating high penetration of renewables sources. *IEEE Syst. J.* **2014**, *PP*, 1–10. [CrossRef]

31. Bergen, R.; Vittal, V. *Power System Analysis*, 2nd ed.; Prentice Hall: Upper Saddle River, NJ, USA, 2006; p. 352.

32. Wood, A.J.; Wollenberg, B.F. *Power Generation, Operation, and Control*, 3rd ed.; John Wiley & Sons: New York, NY, USA, 2013; p. 105.

33. Roytelman, I.; Ganesan, V. Coordinated local and centralized control in distribution management systems. *IEEE Trans. Power Deliv.* **2000**, *15*, 718–724. [CrossRef]

34. Zhu, J. *Optimization of Power System Operation*; John Wiley & Sons: Hoboken, NJ, USA, 2009; p. 409.

35. Paudyal, S.; Canizares, C.A.; Bhattacharya, K. Optimal operation of distribution feeders in smart grids. *IEEE Trans. Ind. Electron.* **2011**, *58*, 4495–4503. [CrossRef]

36. Boyd, S.; Vandenberghe, L. *Convex Optimization*; Cambridge University Press: Cambridge, UK, 2004; pp. 143–150.